



## Design and synthesis of degradation-resistant core–shell catalysts for proton exchange membrane fuel cells

Joon-Ho Koh <sup>a</sup>, Ravikanth Abbaraju <sup>b</sup>, Preethy Parthasarathy <sup>b</sup>, Anil V. Virkar <sup>b,\*</sup>

<sup>a</sup> Materials and Systems Research, Inc., 5395 W 700 S, Salt Lake City, UT 84106, USA

<sup>b</sup> Department of Materials Science and Engineering, University of Utah, Salt Lake City, UT 84112, USA



### HIGHLIGHTS

- Synthesized Ag@Pt core–shell catalysts.
- Investigated their performance in PEM fuel cells.
- Surface tensile stress increases catalyst stability.

### ARTICLE INFO

#### Article history:

Received 6 January 2014

Received in revised form

27 February 2014

Accepted 21 March 2014

Available online 27 March 2014

#### Keywords:

PEM

Proton exchange membrane fuel cells

Core–shell catalysts

Degradation-resistant catalysts

### ABSTRACT

Core@shell catalysts supported on carbon with Ag core and Pt shell were synthesized by a chemical process. EDX spectra confirmed the formation of Ag@Pt core–shell catalysts. High resolution transmission electron microscopy (HRTEM) revealed that the Pt-shell was epitaxially matched to the Ag core. Electrochemical tests on proton exchange membrane (PEM) fuel cells made with Ag@Pt core–shell catalysts as cathode exhibited comparable performance to cells made using commercial Pt–Co-based catalysts as cathodes. Theoretical work suggested that Ag@Pt catalysts should be more stable in the PEMFC applications compared to monolithic Pt catalysts because Pt shell in Ag@Pt catalysts exhibits lower chemical potential of Pt than in monolithic Pt catalysts, thus reducing tendency for dissolution and Ostwald ripening. Lower chemical potential of Pt in the shell is attributed to larger lattice parameter of Ag compared to Pt, which puts the Pt shell in biaxial tension or reduced biaxial compression as compared to monolithic Pt catalysts. Preliminary out-of-cell tests show Ag@Pt catalysts to be stable in an environment containing ionic platinum.

© 2014 Elsevier B.V. All rights reserved.

### 1. Introduction

It is well known that greater catalyst degradation occurs at the cathode of a PEMFC than at the anode even though both anode and cathode may substantially be of the same composition and structure [1–10]. Higher oxygen chemical potential at the cathode is one of the reasons for this higher degradation rate, which results in dissolution of Pt. The three well known modes of Pt dissolution and degradation are: (a) Ostwald ripening [4], (b) Agglomeration/sintering, and (c) Dissolution at the cathode, transport into the membrane, and precipitation into the membrane [6]. Catalyst degradation by growth occurs by a coupled process involving parallel transport of  $Pt^{2+}$  ions through the aqueous medium/ionomer and of electrons through the carbon support [11]. All those factors

which increase the chemical potential of Pt,  $\mu_{Pt}$ , increase the tendency for its dissolution, and thus increase the propensity for degradation. One of the approaches to suppressing catalyst degradation is to alloy Pt with other non-noble metals. An example is Pt–Co alloys, in which the chemical potential of Pt is lowered through alloy formation and/or intermetallic compound/alloy formation. This approach also lowers the net Pt loading, thus potentially lowering cost. Another approach to lowering the Pt loading is to form core shell catalysts in which the core consists of a non-noble metal or an alloy of a non-noble metal (e.g. Cu or Co) with Pt, and a thin shell of Pt formed over the core.

Considerable work has been reported on the synthesis of core–shell catalysts and their catalytic activity [12–16]. Some experimental work has also been reported on their stability, primarily by conducting cyclic voltammetry. Typical cyclic voltammetry tests for durability, although conducted for thousands of cycles, only correspond to a few hours and thus do not represent effects of long term exposure experienced in actual PEMFC cells and stacks. Also,

\*Corresponding author. Tel.: +1 801 581 5396; fax: +1 801 581 4816.

E-mail address: [Anil.virkar@utah.edu](mailto:Anil.virkar@utah.edu) (A.V. Virkar).

little by way of fundamental basis that determines their stability in a fuel cell environment has been reported. A convenient approach involves examining the thermodynamics and the kinetics of Pt dissolution. The process of catalyst particle growth can be described as involving the dissolution of smaller particles and the growth of larger particles. Thus transport occurs from a particle of radius  $r_1$  to a particle of  $r_2$  (where  $r_2 > r_1$ ) and the corresponding thermodynamic driving force for catalyst growth is given by

$$\mu_{\text{Pt}}(r_1) - \mu_{\text{Pt}}(r_2) \quad (1)$$

All those factors which increase the driving force,  $\mu_{\text{Pt}}(r_1) - \mu_{\text{Pt}}(r_2)$ , increase the degradation rate; and all those factors which decrease  $\mu_{\text{Pt}}(r_1) - \mu_{\text{Pt}}(r_2)$ , lower the degradation rate. The chemical potential of Pt also determines the Pt-ion concentration in the liquid/ionomer, which directly affects the kinetics of transport and thus degradation. Alloy catalysts thus may be expected to exhibit greater stability since the chemical potential of Pt in an alloy is lower than in pure Pt. However, other factors may often dictate their stability; for instance, selective etching (dissolution) of the non-noble metal may change the composition and thus change the thermodynamics. Such a process may also lead to in-situ formation of core–shell catalysts, which has been documented in several recent studies. Another important factor that is expected to affect the chemical potential is the presence of mechanical stress. For a material under a hydrostatic pressure,  $p$ , the chemical potential is given by Ref. [17]

$$\mu = \mu(0) + pV_m \quad (2)$$

where  $\mu(0)$  is the chemical potential under zero (negligible) pressure and  $V_m$  is the partial molar volume. In core–shell catalysts, the lattice parameters of the shell (e.g. Pt) and the core in general are different. In some instances, core–shell catalysts with core and shell exhibiting different crystal structures have been explored. The present discussion is restricted to materials in which both the core and the shell have the same crystal structure, namely f.c.c. Thus, the possible elemental materials as candidates for the core are Ag, Au, Cu, Ni, Pd, etc. and their alloys. When both core and shell have the same crystal structure, epitaxial matching of the lattice planes is possible. Since the lattice parameters of the core and the shell are different, a state of stress is developed in both the shell and the core. If the lattice parameter of the core,  $a_{\text{core}}$ , is smaller than that of Pt,  $a_{\text{Pt}}$ , the Pt shell is in a state of biaxial compression, resulting in a positive pressure in the shell ( $p > 0$ ) as compared to a monolithic Pt catalyst of the same size. In such a case, the chemical potential of Pt in the shell is greater than that in a corresponding monolithic (pure) Pt catalyst of the same size. This should increase the tendency for catalyst degradation. We know that  $a_{\text{Cu}}$ ,  $a_{\text{Ni}}$ , are smaller than  $a_{\text{Pt}}$ . So it is the prediction that core–shell catalysts with Cu or Ni as the core will degrade faster than monolithic Pt catalysts of the same size. We also know that  $a_{\text{Ag}}$  and  $a_{\text{Au}}$  are larger than  $a_{\text{Pt}}$ . Thus, core–shell catalysts with Ag or Au as the core and Pt as the shell should create a biaxial tension (or reduced compression) in the Pt shell thus resulting in a negative pressure (or reduced positive pressure) in the shell ( $p < 0$ ). In such a case, the chemical potential of Pt in the shell will be lower than that corresponding to a monolithic Pt catalyst of the same size. Such core–shell catalysts should thus be more resistant to degradation. In terms of the state of stress, the difference in chemical potentials of Pt between a monolithic Pt catalyst and a core–shell catalyst of the same size is given by Ref. [18,19]

$$\Delta\mu_{\text{Pt}}(r) = -\left(\frac{2\sigma_{\theta\theta}}{3}\right)V_m \quad (3)$$

where  $\sigma_{\theta\theta}$  is the circumferential stress created in the shell due to lattice parameter mismatch ( $\sigma_{\theta\theta} > 0$  for tensile). Fig. 1 shows a schematic of the state of stress in such a core–shell catalyst. The expected improvement in stability can be described in terms of electric potential,  $\Delta\phi$ , given by

$$\Delta\phi = -\frac{\Delta\mu_{\text{Pt}}(r)}{2F} = \left(\frac{\sigma_{\theta\theta}}{3F}\right)V_m \quad (4)$$

In the case of Ag-core/Pt-shell catalyst, the expected improvement in stability is  $\sim 190$  mV, both based on thermodynamic calculations and the density functional theory (DFT) calculations [18,20].

In the present manuscript, we describe the synthesis and preliminary characterization of Ag-core/Pt-shell catalysts for PEMFC. The approach consisted of using commercial Ag-catalyst supported on high surface area carbon. The surface and the near surface layers are replaced by Pt via a displacement reaction by simply immersing the supported Ag catalyst in a Pt-salt solution. Since Pt is more noble than Ag, the following displacement reaction is expected



That is, two surface Ag atoms are dissolved for one Pt deposited. The preceding assumes that Pt ions participating in the reaction are divalent. Fig. 2 shows a schematic of the displacement reaction. A similar approach was used to synthesize Pt–Co-core/Pt-shell catalyst starting with commercial Pt–Co catalyst supported on carbon (E-TEK C14-20/C<sup>–1</sup>). In the case of Pt–Co alloy catalysts, when placed in a Pt-ion solution, the expected displacement reaction is given by



Catalyst characterization was conducted by transmission electron microscopy (TEM). Membrane Electrode Assemblies (MEAs) were made with Pt-salt treated and untreated catalysts and their performance was evaluated. Preliminary stability tests were conducted ex-situ by placing the synthesized core–shell catalysts in a Pt-salt containing electrolyte solution.

## 2. Experimental procedure

Silver nanocatalysts supported on carbon were purchased from BASF Fuel Cell, Inc. (Somerset, NJ). This commercial nanocatalyst (Cat. No. C8-20) has an average particle size of  $\sim 5$  nm. The silver catalyst was mixed with a dilute aqueous solution of  $\text{PtCl}_4$  ( $0.1 \text{ g L}^{-1}$ ) without any other chemical agents. The atomic ratio of platinum to silver in the slurry mixture was approximately 1:19. The low ratio of Pt/Ag was intended to create a thin layer (ideally monolayer) of Pt-shell over the silver nano particles. The mixture was placed in an ultrasonic bath at room temperature. The time of mixing in an ultrasonic bath was varied from 5 to 570 min. After the mixing, the slurry was filtered and washed with deionized water. Then it was dried at  $50\text{--}60^\circ\text{C}$ . Also, the displacement reaction was conducted at two temperatures,  $20^\circ\text{C}$  and  $60^\circ\text{C}$ .  $\text{PtCl}_4$  was used instead of  $\text{PtCl}_2$  because of its higher solubility. However, the anticipated displacement reaction still involves  $\text{Pt}^{2+}$  since a small concentration of  $\text{Pt}^{2+}$  exists in the solution, especially once Pt is formed due to the local reaction  $\text{Pt} + \text{PtCl}_4 \rightarrow 2\text{PtCl}_2$  [18]. The samples were characterized by transmission electron microscopy (TEM). Micro-chemical analysis was performed by EDX. In addition, X-ray photoelectron spectroscopy (XPS) spectra were obtained from the core and the shell regions.

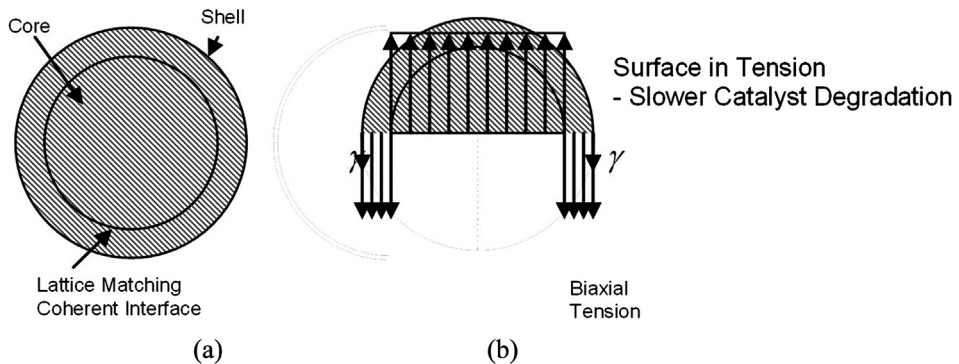


**Fig. 1.** (a) A schematic of a core–shell catalyst. (b) A free body diagram showing the stress distribution in the shell and the core. The shell is either under a biaxial tension or under a reduced biaxial compression if the core is Ag and the shell is Pt.

MEAs were fabricated using Nafion 115 membranes and tested to determine their performance using the following procedure. Membrane electrode assemblies (MEAs) were fabricated using commercial (Fuel Cell Store, CO) gas diffusion solid polymer electrolyte electrode (GDE) with double sided coatings (ELAT GDE HT 140E-W). The anode specifications were as follows: Pt loading  $5 \text{ g m}^{-2}$  with 30% Pt on Vulcan XC-72 as the catalyst. Four different cathodes were used: (a) Commercial Pt–Co catalyst supported on carbon (E-TEK C14-20/C<sup>-1</sup>). (b) Commercial Ag catalysts supported on carbon (E-TEK C8-20). (c) Commercial Ag catalysts supported on carbon treated in a  $\text{PtCl}_4$  + dimethyl sulfoxide (DMSO) solution. (d) Commercial Pt–Co catalysts supported on carbon treated in a  $\text{PtCl}_4$  + DMSO solution. MEAs were prepared by pressing the electrodes on the membrane in a Carver hot press at  $90^\circ\text{C}$  under a pressure of  $\sim 7 \text{ MPa}$  for 5 min. All MEAs were fabricated using commercial Nafion 115 membranes.

### 2.1. Fuel cell testing

Teflon gas-sealing gaskets were used to clamp and secure the MEAs into a commercial (Fuel Cell Technologies, Inc.)  $5 \text{ cm}^2$  fuel cell test stand. The load used was Decade Resistor (PPM, Inc., OH) and the corresponding voltage and current data were obtained using Keithley Instruments digital multimeter (Model 2000). The cell was fed with humidified  $\text{H}_2$  and  $\text{O}_2$ . Required humidification was achieved by bubbling  $\text{H}_2$  and  $\text{O}_2$  gases through conical flasks immersed in a temperature controlled water bath. Both the fuel ( $\text{H}_2 + \text{H}_2\text{O}$ ) and the oxidant ( $\text{O}_2 + \text{H}_2\text{O}$ ) pressures were maintained slightly above 1 atm. The MEAs in all tests were maintained at  $80^\circ\text{C}$ . Before obtaining polarization data, the cell was equilibrated at a cell

voltage of about 0.4 V for 3–4 h with humidified  $\text{H}_2$  (purity 99.99%) on the anode and humidified  $\text{O}_2$  (purity 99.9%) on the cathode until a steady current was achieved. The polarization curves were swept from top to down, with current density being measured from zero (at OCV) to the highest measured. The data points were collected manually using a load box with a residence time of about 5 min at each current density.

The main objective of fuel cell testing was to compare the performance of similarly made MEAs using commercial Pt–Co catalysts, Ag-catalysts, and synthesized Ag-core/Pt-shell catalysts. Experiments were also conducted on commercial Pt–Co (E-TEK) catalysts supported on carbon treated in a  $\text{PtCl}_4$  solution. As given in Eq. (6), the expectation was that the displacement reaction will occur such that some of the cobalt from Pt–Co will be replaced by Pt thus forming a core–shell catalyst with Pt–Co as the core and Pt as the shell. Some of the as-synthesized Ag-core/Pt-shell catalysts were immersed in a  $\text{PtCl}_4$  solution in water containing  $0.1 \text{ g L}^{-1}$  and maintained at a temperature between  $50^\circ\text{C}$  and  $60^\circ\text{C}$  for 10 days. The objective was to determine the possible growth of catalysts particles.

### 3. Results and discussion

Fig. 3 shows a high resolution transmission electron micrograph (HRTEM) of the as-synthesized Ag-core/Pt-shell catalyst particle. The lattice image of the catalyst particle shows that the lattice planes are contiguous between the core and a possible shell. Fig. 4 shows XPS spectra obtained from the core–shell catalyst and from a standard Pt reference. A small amount of dry catalyst powder sample was loaded and placed inside the XPS chamber. After

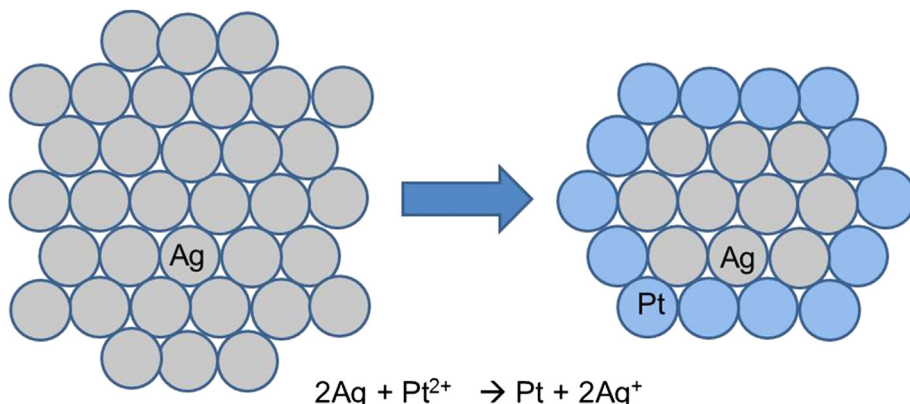


**Fig. 2.** A schematic of the displacement reaction used for forming Ag-core/Pt-shell catalysts.

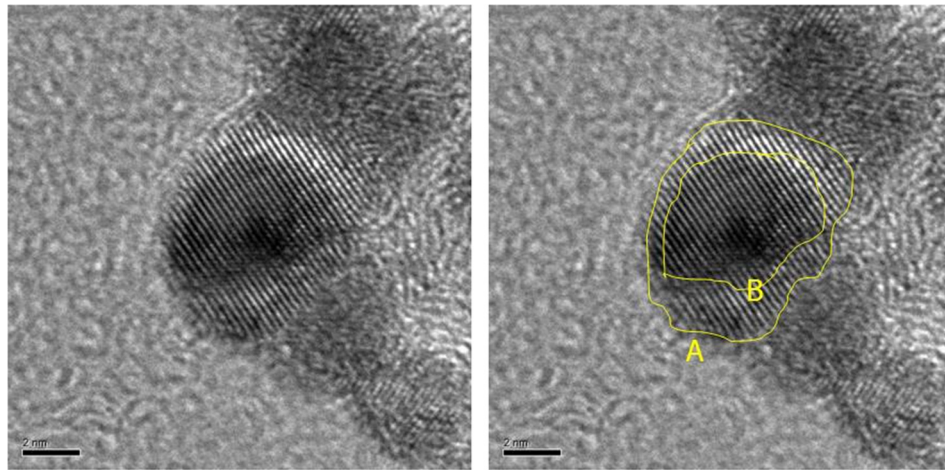


**Fig. 3.** HRTEM images of the as-synthesized Ag-core/Pt-shell catalysts. Both micrographs are of the same region. The micrograph on the left shows the contiguous lattice planes from the inner core through the outer shell indicating good epitaxial matching. The right micrograph shows the approximate delineation of the shell from the core.

reaching a base pressure of  $10^{-9}$  torr, analysis was carried out by scanning from 1200 eV to 0 eV. The copper (sample holder) peak observed at 962 eV was not included in the spectrum. Note that the peaks corresponding to binding energies of 74.6 eV and 71.3 eV observed in the standard Pt reference are also observed in the XPS spectra obtained from the core–shell catalyst. This shows that part of the Ag was replaced by Pt by the displacement reaction.

The XPS spectra in Fig. 4 show that a layer of Pt was formed. However, these spectra cannot unequivocally confirm the formation of a core–shell structure. In order to determine if indeed a core–shell structure is formed, micro-chemical analysis was performed on the synthesized catalysts. The EDX spectra in Fig. 5 show that the Ag peak is larger from the center of the particle than from the shell area. This confirms the formation of a core–shell catalyst.

Fig. 6 shows the results of MEA testing. In all tests, the anode was 30% Pt-supported on carbon from E-TEK. Fig. 6(a) compares the performance of two MEAs; one made with commercial Pt–Co/C catalyst as the cathode and the other made with commercial Ag/C as the cathode. As seen in the figure, the performance of the MEA with Pt–Co/C catalyst is superior. It is interesting to note, however, that reasonable performance was also measured with Ag/C as the cathode. These were short term tests and thus long term stability of

MEA with Ag/C as the cathode is not known. It is expected that the Ag/C catalysts will likely degrade. Fig. 6(b) compares the performance of MEAs made using: (i) As-synthesized Ag-core/Pt-shell catalysts (60 min at 20 °C), (ii) As-synthesized Ag-core/Pt-shell catalysts (60 min at 60 °C), and (iii) As-synthesized Pt–Co-core/Pt-shell catalysts (60 min at 20 °C). As seen in the figure, the performance of all three MEAs is virtually identical. This suggests that the catalytic activity of all three cathode catalysts, which are core/shell catalysts (but with different core in one of them), exhibit nearly identical behavior. Since no measurements of catalyst surface areas were made, possible differences related to different areas are not addressed here.

The performance of all MEAs tested in the present work is somewhat lower than performance levels observed in typical PEM tests. However, it should be noted that the typical particle size of the Ag-catalyst was  $\sim 5$  nm or even slightly greater. By contrast, catalyst particle size in most commercial, monolithic Pt-catalyst supported on high surface area carbon is on the order of 2 nm [21]. That is the typical catalyst surface area of the state-of-the-art Pt catalyst is over two and half times larger. The observed lower open circuit voltage and lower performance in the present work is thus believed to be due to the cathode catalyst particle being much

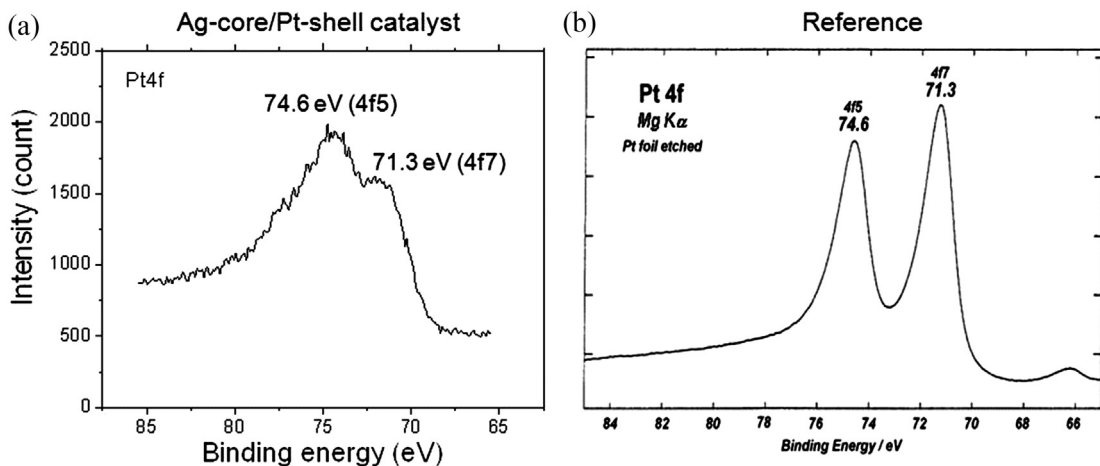


**Fig. 4.** (a) XPS spectra obtained on Ag-core/Pt-shell catalysts synthesized by the displacement reaction. (b) XPS spectra from a platinum reference. Both representative peaks are observed in the core/shell catalysts.

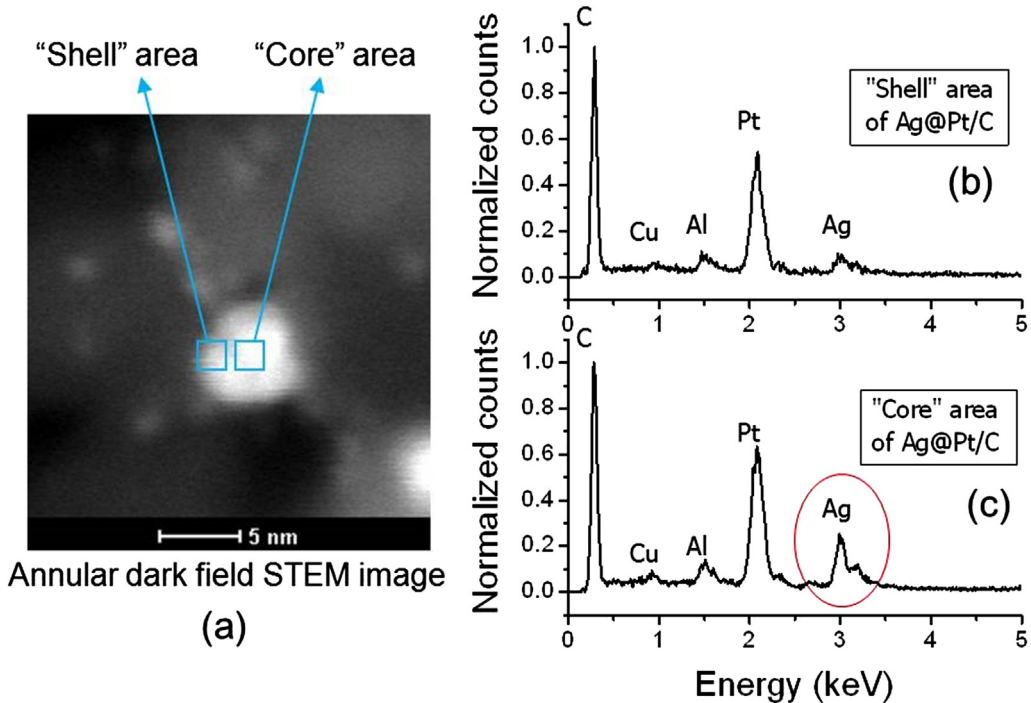
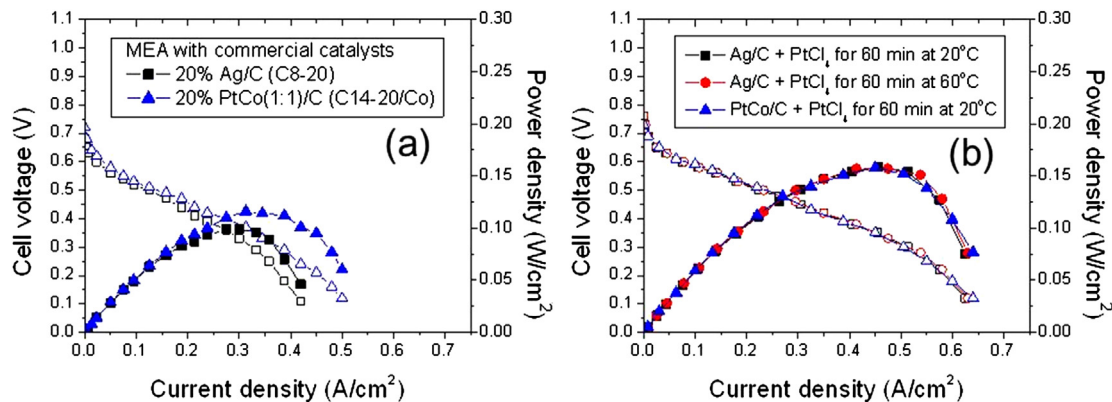


**Fig. 5.** (a) A TEM dark field image of the synthesized Ag-core/Pt-shell catalyst. Chemical analysis was performed in the center and near the periphery of the particle. (b) EDX spectra obtained from the shell area showing a large Pt peak and a small Ag peak. (c) EDX spectra obtained from the core area. The Ag peak in (c) is larger than in (b).

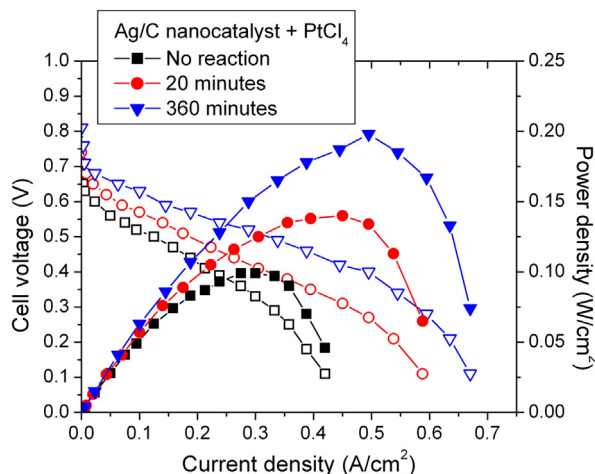
larger than the state-of-the-art Pt catalyst. No transmission electron microscopy was done on the Pt–Co (E-TEK C14-20/C<sup>−1</sup>) catalysts. The relatively low performance observed with the Pt–Co catalyst is thus may also likely be due to non-optimum catalyst size. In fact, experimental work on Pt alloy catalysts from the same vendor (E-TEK) has shown that the Pt-alloy particles are larger in size than monolithic Pt catalysts [22]. Preliminary results nevertheless show that core–shell catalysts with Ag as the core yield results comparable to catalysts with Pt-alloy as the core. Also note that the performance of MEAs with core/shell catalysts (Fig. 6(b)) is slightly superior to the performance of MEA made with the as-received Pt–Co alloy catalysts.

Fig. 7 compares the performance of MEAs with Ag-core/Pt-shell catalysts made with different displacement reaction times ranging between 0 min (as-received, so no Pt shell) and 360 min. Note that the highest performance was measured with the catalyst that was

treated for 360 min. It is likely that the corresponding Pt-shell was the thickest and/or the longer treatment time resulted in a more complete Pt coverage. It is expected that beyond some treatment time, no further improvement will occur as a saturation level reaches. In fact, it was observed that the performance of cells made with catalyst treated for 570 min was slightly lower than catalyst treated for 360 min. Also, the present approach should naturally restrict the shell thickness to a few atomic layers, beyond which the reaction will shut down due to sluggish solid state diffusion through the shell at such low temperatures. Fig. 7 also shows that the open circuit voltage for the MEA with the as-received Ag/C catalyst was ~0.65 V but that for the MEA made with catalyst treated in PtCl<sub>4</sub> solution for 360 min was ~0.82 V. This too suggests that the initial drop in voltage observed is primarily associated with cathode polarization and that the generally lower performance observed in the present work is attributed to the relatively large



**Fig. 6.** (a) Voltage vs. current density traces obtained on MEAs made using the as-received Ag/C catalyst and the as-received Pt–Co/C catalyst. The results show that the MEA performance with PtCo catalyst is superior. (b) Voltage vs. current density traces obtained with MEAs made using Ag-core/Pt-shell catalysts synthesized at 20 °C and 60 °C for 60 min, and using Pt–Co-core/Pt-shell catalyst synthesized at 20 °C for 60 min.



**Fig. 7.** Performance of MEAs made with Ag-core/Pt-shell catalysts made with different displacement reaction times during the synthesis.

particle size ( $\sim 5$  nm) of the Ag/C catalyst compared to state-of-the-art Pt/C catalyst (which is typically  $\sim 2$  nm).

Catalyst durability is typically studied by conducting accelerated testing by cyclic voltammetry. For example, Ohashi et al. [23] investigated catalyst stability of Pt–Pd catalysts by cyclic voltammetry by conducting 30,000 cycles between 0.6 V and 1.0 V at a rate of  $100\text{ mV s}^{-1}$ . This corresponds to a total test time of only 67 h. Also, the  $\text{Pt}^{2+}$  ion concentration varies over a range between the two voltages. For example, according to Darling and Meyers [24], the  $\text{Pt}^{2+}$  ion concentration varies between  $\sim 10^{-7}\text{ M}$  and  $\sim 10^{-4}\text{ M}$  between 0.4 V and 1.2 V. Thus, in such cyclic tests, the actual time

the electrode is exposed to high  $\text{Pt}^{2+}$  ion concentration is considerably lower than the total test duration (much lower than the total time of 67 h of cyclic voltammetry in the work of Ohashi et al. [23]). In the present work, durability studies were instead conducted in a static environment containing a fixed concentration of platinum ions for a much longer time. Fig. 8 shows TEM images of the as-synthesized Ag-core/Pt-shell catalysts and after 10 days (240 h) in  $0.1\text{ g L}^{-1}\text{ PtCl}_4$  solution in water (the same concentration as used for forming Ag@Pt catalysts by the displacement reaction). Preliminary results show that no detectable growth occurred. Longer term experiments with measurements of particle size and size distributions will be necessary to determine how significant is the improvement in catalyst durability. Also, similar experiments need to be conducted on monolithic Pt-catalysts supported on carbon. Nevertheless, the present studies in which catalyst particles were tested for 240 h in  $\text{PtCl}_4$  appear to be of at least comparable severity as the cyclic voltammetry tests typically conducted for catalyst durability studies. The present studies thus demonstrate that Ag-core/Pt-shell catalysts are possible candidates as cathode for PEMFC.

#### 4. Summary

Carbon-supported core–shell catalysts with Ag and Pt–Co alloys as the core and Pt as the shell were synthesized by a displacement reaction. The as-synthesized Ag-core/Pt-shell catalysts were characterized by HRTEM, EDX and XPS. The Pt-shell was epitaxially matched to the Ag core. MEAs were fabricated and tested. The performance of the MEAs with Ag-core/Pt-shell catalysts was about the same as with Pt–Co–core/Pt–shell catalysts, and superior to the performance of MEAs made using the as-received Pt–Co–catalysts. Preliminary ex-situ studies showed that Ag-core/

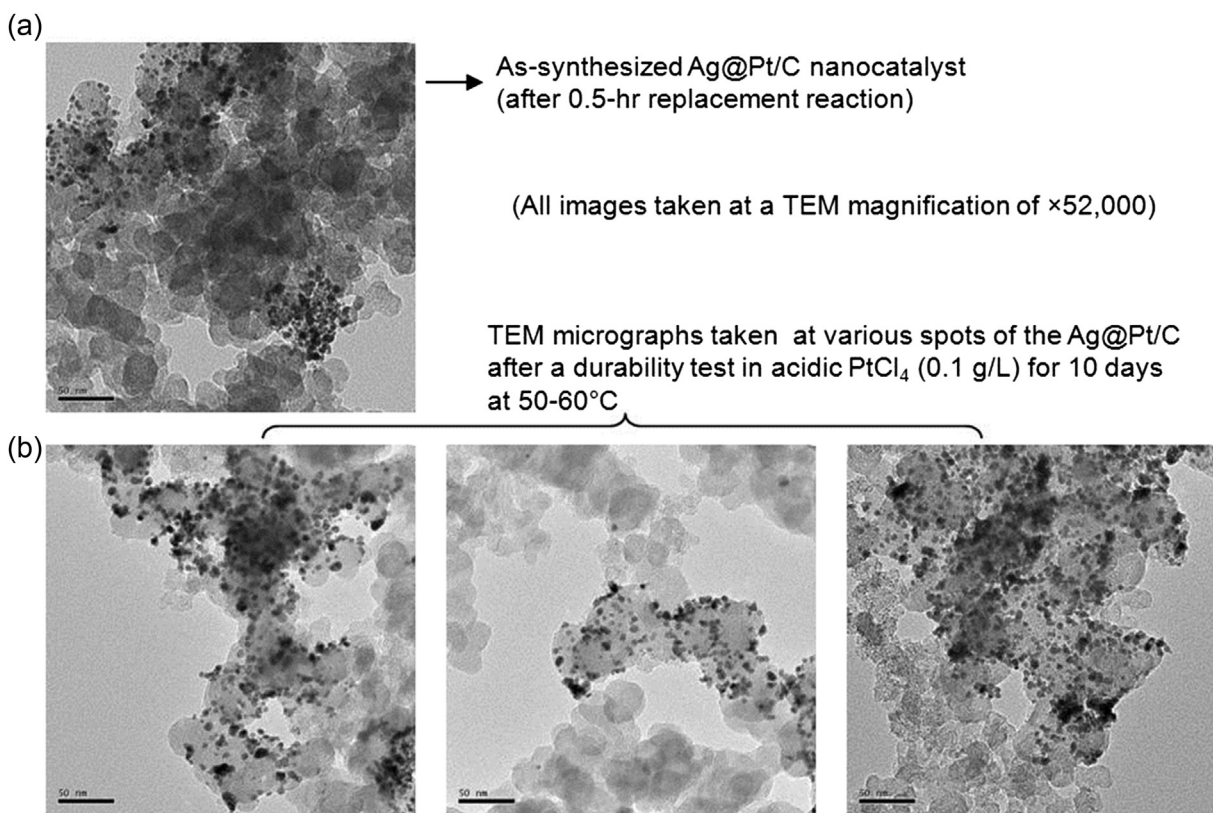


**Fig. 8.** (a) A TEM micrograph of the as-synthesized Ag-core/Pt-shell catalyst supported on carbon. (b) Three TEM micrographs of the Ag-core/Pt-shell catalysts immersed in a  $\text{PtCl}_4$  ( $0.1\text{ g L}^{-1}$ ) aqueous solution for 10 days at  $\sim 50\text{--}60^\circ\text{C}$ .

Pt-shell catalysts exhibited negligible growth in 10 days when immersed in a Pt ion containing solution. The stability of Ag-core/Pt-shell catalysts is attributed to the creation of a biaxial tensile stress in the Pt shell due to the larger lattice parameter of Ag compared to Pt [18,19]. The present work shows that Ag-core/Pt-shell catalysts are potential candidates as cathode for PEMFC.

## Acknowledgements

The work at the University of Utah was supported in part by the National Science Foundation under Grant No. CBET-0931080 (Preethy Parthasarathy's work), U.S. Department of Energy under Grant Number DE-FG02-06ER46086 (R. Abbaraju's and Anil Virkar's work), and in part by the U.S. Department of Energy, Office of Science, Office of Basic Energy Sciences under Award Number DE-SC0001061 as a flow-through from the University of South Carolina (Preethy Parthasarathy's and Anil Virkar's work). The work at Materials and Systems Research, Inc. was funded by a DOE-SBIR Phase I Grant DE-FG02-08ER85122 (Joonho Koh's work).

## References

- [1] M.S. Wilson, F.H. Garzon, K.E. Sickhaus, S. Gottesfeld, *J. Electrochem. Soc.* 140 (1993) 2872–2877.
- [2] R. Ornelas, A. Stassi, E. Modica, A.S. Arico, V. Antonucci, *ECS Trans.* 3 (2006) 633–641.
- [3] X. Wang, R. Kumar, D. Meyers, *Electrochem. Solid State Lett.* 9 (2006) A225–A227.
- [4] J. Xie, D.L. Wood III, K.L. More, P. Atanassov, R.L. Borup, *J. Electrochem. Soc.* 152 (2005) A1011–A1020.
- [5] P.J. Ferreira, G.J. Lao, Y. Shao-Horn, D. Morgan, R. Makaharia, S. Kocha, H.A. Gasteiger, *J. Electrochem. Soc.* 152 (2005) A2256–A2271.
- [6] W. Bi, G.E. Gray, T.F. Fuller, *Electrochem. Solid State Lett.* 10 (2007) B101–B104.
- [7] K. Yasuda, A. Taniguchi, T. Akita, Z. Siroma, *Phys. Chem. Chem. Phys.* 8 (2006) 746–752.
- [8] A. Ohma, S. Suga, S. Yamamoto, K. Shinohara, *ECS Trans.* 3 (2006) 519–529.
- [9] H. Liu, J. Zhang, F.D. Coms, W. Gu, B. Litteer, H.A. Gasteiger, *ECS Trans.* 3 (2006) 493–505.
- [10] B. Merzougui, S. Swathirajan, *J. Electrochem. Soc.* 153 (2006) A2220–A2226.
- [11] A.V. Virkar, Y. Zhou, *J. Electrochem. Soc.* 153 (2007) B540–B547.
- [12] J. Zhang, F. Lima, M. Shao, K. Sasaki, J. Wang, J. Hanson, R. Adzic, *J. Phys. Chem. B* 109 (2005) 22701–22704.
- [13] S. Yamamoto, U.S. Patent 7,205,255, April 17, 2007.
- [14] W. Zhou, J.Y. Yee, *Electrochem. Commun.* 9 (2007) 1725–1729.
- [15] Y. Ma, P.B. Balbuena, *J. Electrochem. Soc.* 157 (2010) B959–B963.
- [16] S. Koh, J. Leich, M.F. Toney, P. Strasser, *J. Phys. Chem. C* 111 (2007) 3744–3752.
- [17] O.F. Devoreaux, *Topics in Metallurgical Thermodynamics*, John Wiley-Interscience, New York, 1983.
- [18] P. Parthasarathy, A.V. Virkar, *J. Power Sources* 196 (2011) 9204–9212.
- [19] A.V. Virkar, U.S. Patent 8,168,561 B2, May 1, 2012.
- [20] G.E. Ramirez-Caballero, Y. Ma, R. Callejas-Tovar, P.B. Balbuena, *Phys. Chem. Chem. Phys.* 12 (2010) 2209–2218.
- [21] P. Parthasarathy, A.V. Virkar, *J. Power Sources* 234 (2013) 82–90.
- [22] H.R. Colon-Mercado, B.N. Popov, *J. Power Sources* 155 (2006) 253–263.
- [23] M. Ohashi, K.D. Beard, S. Ma, D.A. Blom, J. St-Pierre, J.W. Van Zee, J.R. Monnier, *Electrochim. Acta* 55 (2010) 7376–7384.
- [24] R.M. Darling, J.P. Meyers, *J. Electrochem. Soc.* 150 (11) (2003) A1523–A1527.